Supporting Information

Improving acceptor efficacy rather than energy transfer efficiency: Dominant contribution of monomers of the acceptors modified on upconversion nanoparticles

Jie Ren[a], Yadan Ding[a,*], Hancheng Zhu[a], Zhipeng Li[a], Xia Hong[a,**], Huiying Zhao[b], Hong Zhang[c]

[a]*Key Laboratory of UV-Emitting Materials and Technology (Northeast Normal University), Ministry of Education, Changchun 130024, China*

[b]*Department of Basic Medicine, Gerontology Department of First Bethune Hospital, University of Jilin, Changchun, Jilin 130021, China*

[c]*Van't Hoff Institute for Molecular Sciences, University of Amsterdam, Science Park 904, 1098 XH Amsterdam, The Netherlands*

[*]Corresponding author.

[**]Corresponding author.

E-mail addresses: dingyd044@nenu.edu.cn (Y. Ding), xiahong@nenu.edu.cn (X. Hong)

Table of contents:

1. Materials and synthesis methods

1.1. Materials

YCl_3 (99.99%), $YbCl_3$ (99.9%), $ErCl_3$ (99.99%), oleic acid (OA, 90%), 1-Octadecene (ODE, 90%), poly (allylamine) solution (PAAM, 20 wt%, Mw~17,000), rose bengal (RB, 95%), 6-bromohexanoicacid (97%), N-(3-dimethylaminopropyl)-N'-ethylcarbodiimide hydrochloride (EDC, premium), N-hydroxysulfosuccinimide sodium salt (NHS, >98%) and 1,3-diphenylisobenzofuran (DPBF) were purchased from Sigma-Aldrich. NaOH (>90%) was purchased from Merck KGaA, and NH_4F (>98.0%) was from Alfa Aesar. Dulbecco's modified eagle's medium (DMEM), trypsin and bovine fetal blood serum (FBS) were purchased from Gibco. Cell Counting Kit-8 (CCK-8) reagent was from Dojindo. Glutaraldehyde (50%) was purchased from Tianjin Guangfu Fine Chemical Industry Research Institute. 2′,7′-Dichlorodihydrofluorescein diacetate (DCFH-DA, 97%) was purchased from Macklin. Calcein-AM/propidium iodide (PI) Double Stain Kit was obtained from KeyGEN BioTECH. All the other solvents were of analytical grade and used as received without further purification.

1.2. Synthesis of $NaYF_4$: Yb^{3+}, Er^{3+} UCNPs

The $NaYF_4$: Yb^{3+}, Er^{3+} UCNPs synthesized according to the reported protocol.[1,2] The whole process was performed under the protection of nitrogen flow and vigorous magnetic stirring. Firstly, YCl_3 (0.78 mmol), $YbCl_3$ (0.20 mmol) and $ErCl_3$ (0.02 mmol) were mixed in OA (6 mL) and ODE (15 mL), and the mixture was gradually heated to 160 °C for 30 min. Secondly, when the temperature cooled below 50 °C, 5 mL of methanol solution containing 2.5 mmol of NaOH and 4.0 mmol of NH_4F was added to the mixture immediately. The reaction temperature was then slowly increased to 310 °C and kept for 90 min after evaporating methanol. Next, the samples were washed with cyclohexane and acetone/ethanol when cooling down to room temperature. Finally, the products were dispersed in cyclohexane.

2. TEM and XRD pattern of UCNPs

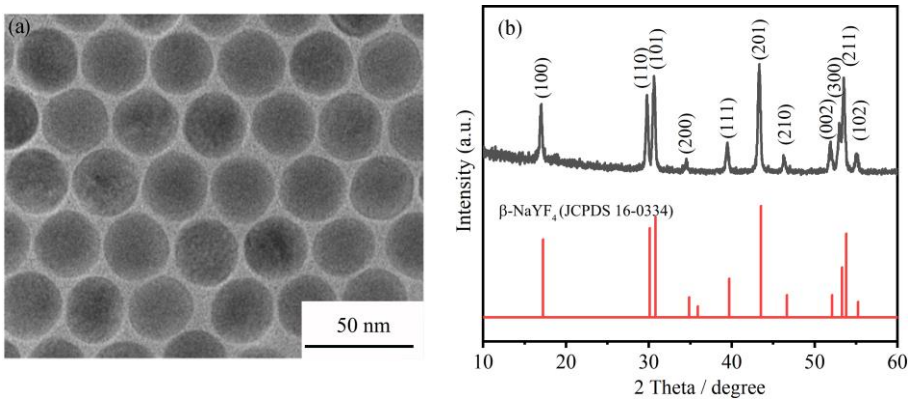

Fig. S1. (a) TEM image and (b) XRD pattern of $NaYF_4$: Yb^{3+}, Er^{3+} UCNPs and the standard diffraction pattern of $NaYF_4$ (JCPDS card no. 16-0334).

3. FTIR spectra and spectral overlap

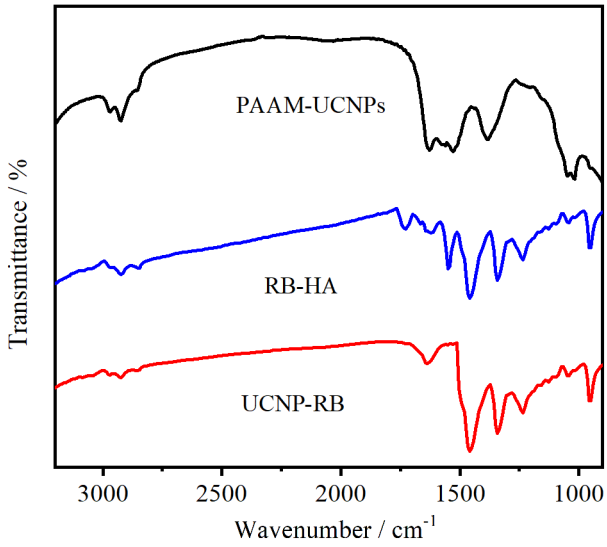

Fig. S2. FTIR spectra of amino-modified UCNPs, carboxyl-modified RB molecules, and the UCNPs-RB nanoconjugates.

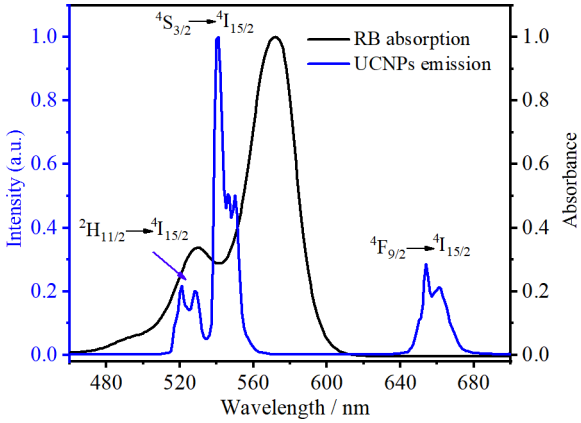

Fig. S3. Spectral overlap between the emission spectrum of the UCNPs and the absorption spectrum of RB molecules.

4. Temporal behaviors of UCNPs-RB and the nonradiative ET efficiency

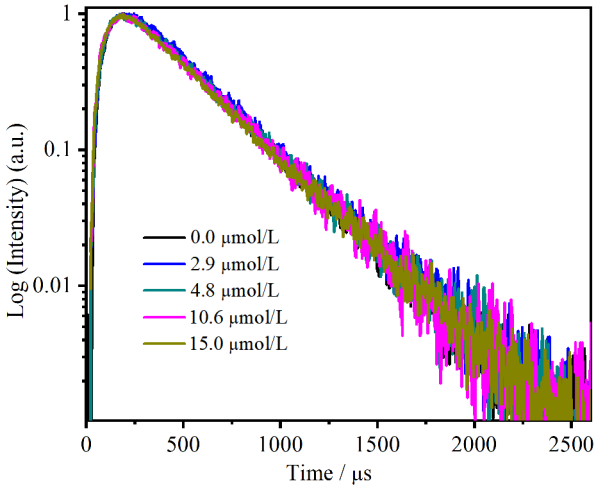

Fig. S4. Temporal behaviors of the UCL from the UCNPs-RB conjugates under 980 nm excitation monitored at 655 nm.

Table S1. The decay lifetimes of the green UCL and the red UCL.

	0.0 μmol/L	2.9 μmol/L	4.8 μmol/L	10.6 μmol/L	15.0 μmol/L
$\tau_{541\ nm}$ / μs	117	114	110	100	95
$\tau_{655\ nm}$ / μs	284	285	283	283	285

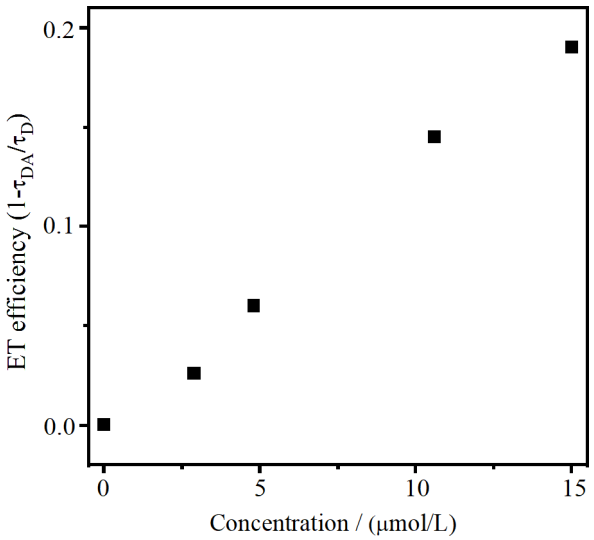

Fig. S5. The nonradiative ET efficiency of the UCNPs-RB conjugates with various amounts of RB calculated according to the decay lifetime of the green UCL.

5. Absorption of the UCNPs-RB conjugates

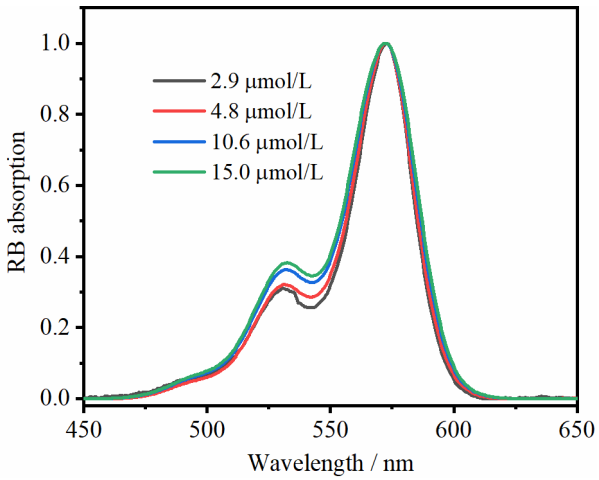

Fig. S6. Normalized absorption spectra of the UCNPs-RB conjugates with various amounts of RB: 2.9 μmol/L, 4.8 μmol/L, 10.6 μmol/L and 15.0 μmol/L.

6. The consumption rate of DPBF (*k*) by linear fitting

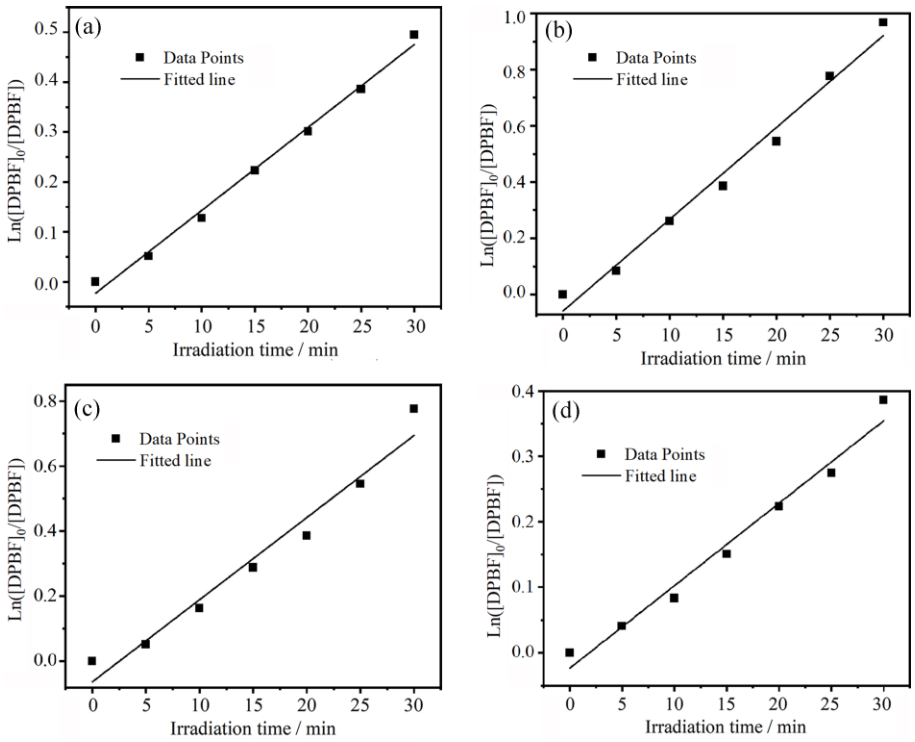

Fig. S7. The fitted line of the DPBF consumption with the increasing exposure time. The UCNPs-RB conjugates with (a) 2.9 μmol/L, (b) 4.8 μmol/L, (c) 10.6 μmol/L and (d) 15.0 μmol/L.

Table S2. The consumption rate of DPBF (*k*) by linear fitting.

RB loading amount on the UCNPs	2.9 μmol/L	4.8 μmol/L	10.6 μmol/L	15.0 μmol/L
k	0.017	0.033	0.025	0.013
R^2	0.992	0.982	0.960	0.974

7. SEM images and UCL spectra of the UCNPs-RB conjugates with and without attached to the cells

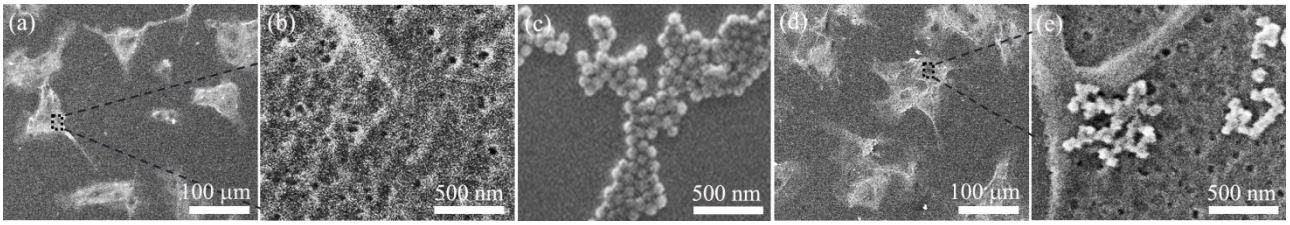

Fig. S8. SEM images of (a, b) the cells, (c) the UCNPs-RB conjugates and (d, e) the cells incubated with the UCNPs-RB conjugates fixed on the silicon slides. (b) and (e) are magnified from the selected areas in (a) and (d), respectively.

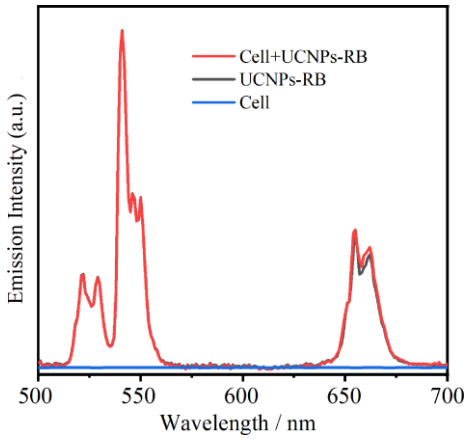

Fig. S9. Emission spectra of the cells, the UCNPs-RB conjugates and the cells incubated with the UCNPs-RB conjugates fixed on the silicon slides.

8. Intracellular ROS production under 532 nm excitation

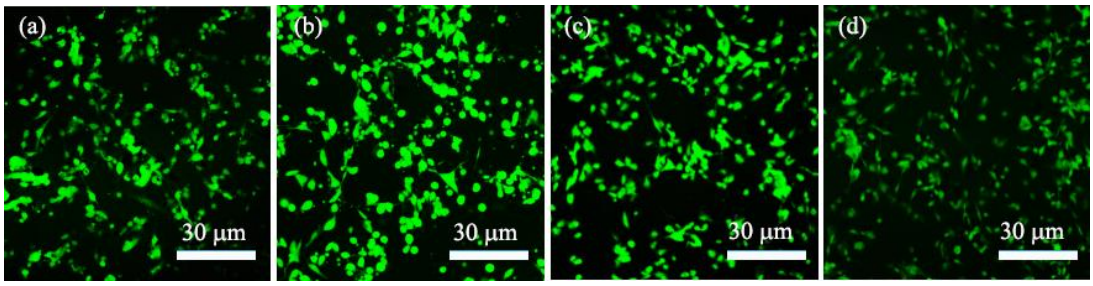

Fig. S10. Detection of ROS produced by the UCNPs-RB conjugates with the RB concentration of (a) 2.9 μmol/L, (b) 4.8 μmol/L, (c) 10.6 μmol/L and (d) 15.0 μmol/L in U87MG cells stained by DCFH-DA under 532 nm excitation.

References

1. Ding YD, Wu F, Zhang YL, Liu XM, Jong ED, Gregorkiewicz T, et al. Interplay between static and dynamic energy transfer in biofunctional upconversion nanoplatforms. *J Phys Chem Lett.* 2015;6:2518.

2. Johnson NJJ, Korinek A, Dong CH, van Veggel FCJM. Self-focusing by Ostwald ripening: a strategy for layer-by-layer epitaxial growth on upconverting nanocrystals. *J Am Chem Soc*. 2012;134:11068.